

## Review

# Stress enhanced environmental corrosion and lifetime prediction modelling in silica optical fibres

P. OSTOJIC

*Photonics Section, Telecommunications Science and Technology Branch,  
Telecom Research Laboratories, Clayton, Victoria, Australia*

The glass/water interaction is reviewed from early experimental work in bulk samples to the current molecular interpretation of bond rupture in that interaction. The significance of that work to static fatigue in silica optical fibres is discussed. Assumptions concerning the basic equations used to predict the rate of crack propagation, and hence, the lifetime of silica optical fibres, are questioned. Issues such as flaw distribution and the true nature of the crack tip are highlighted along with deficiencies in test methods and data analysis techniques used to obtain fibre "lifetime" parameters. These factors have resulted in no single fibre lifetime model becoming universally accepted with some 15 published lifetime models currently available. It is suggested that lifetime theory based on large, well-defined cracks in bulk material is no longer entirely sufficient to explain the static fatigue behaviour of the nanometre-sized flaws found in current optical fibres. Instead, the literature indicates a two-stage model consisting of a precursor stage followed by the currently accepted bond-rupture mechanism, to be more appropriate.

### 1. Introduction

A primary consideration in the design of any system is its longevity and this is particularly true for telecommunications networks. For such networks, accurate estimates of system lifetime are needed to avoid the possibility of high capital expenditure should an unforeseen, premature failure occur.

Current telecommunications networks are based on silica optical fibres which, despite their numerous advantages, have the potential drawback of reacting deleteriously with water when subjected to a tensile stress. This, combined with a number of other factors associated with optical fibres/cable design, manufacturing and operating environment, has resulted in a designed service lifetime of some 40 years for optical fibres, with this figure based on current fibre lifetime models. However, uncertainties, contradictions and a lack of full understanding of the various processes involved have cast some doubt on the accuracy and general applicability of those models.

It is the purpose of this work to present a review of static fatigue in silica optical fibres, highlighting many of the factors known to influence that phenomenon and discussing shortcomings associated with current lifetime models.

### 2. The glass/water interaction

Reports that the strength of glass is dependent on the loading rate used date back to 1899 [1], however the

first detailed study on the effect of environment and composition on the strength of glass was that reported by R. J. Charles in 1958 [2, 3]. Using centreless-ground rods of soda-lime glass, Charles showed the time to failure of such rods under 3-point bending was dependent on temperature with no discernible effect occurring at  $-170^{\circ}\text{C}$ .

Later work by S. M. Wiederhorn and his colleagues [4, 5] using double-cantilever-beam specimens of soda-lime glass, demonstrated that the rate of crack growth in that glass was dependent on both relative humidity and applied tensile stress. Those workers also identified three distinct regions of crack growth rate behaviour in that glass (Fig. 1).

Crack growth rate (velocity) was reported to require a critical minimum stress in soda-lime glass and, once attaining that stress, an increase in crack velocity with applied load resulted (Region I). Crack velocity was also found to depend on relative humidity in this region. In Region II crack velocity was shown to be independent of applied load but dependent on relative humidity while in region III, it was again found to increase with applied load but to be independent of relative humidity.

Subsequent work has shown many materials other than glass exhibit the tri-modal crack growth behaviour shown in Fig. 1 [6–8]. Much of this behaviour may be explained in terms of static fatigue, a term first coined in 1946 as a description of the result of the interaction between glass and water under the

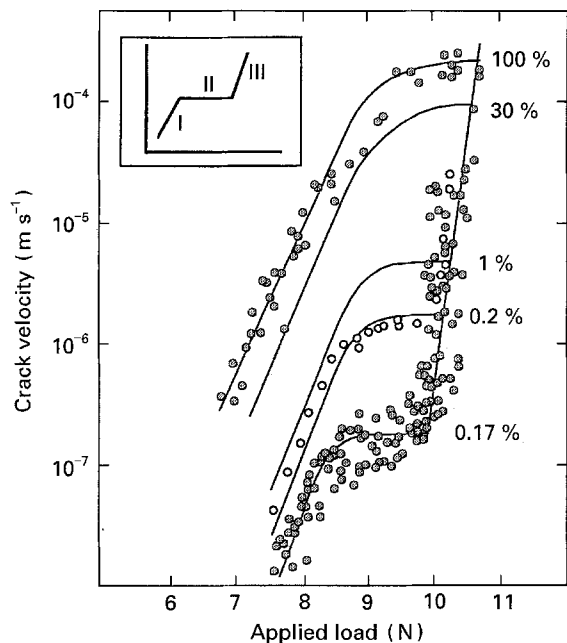


Figure 1 Crack growth rate (velocity) versus applied load for soda-lime glass at different humidities (after [4]). Insert depicts a stylized version of behaviour at a particular humidity and indicates regions I, II and III.

influence of an applied tensile stress [9]. Static fatigue theory suggests that crack motion under the conditions described results from a heterogeneous chemical reaction between the material and environment at the root of the crack tip [10].

In general, a heterogeneous reaction occurring at a surface proceeds in five distinct steps with the slowest step determining the overall rate of the process. The successive stages are [11]:

1. Transport of the gaseous reactants to the surface (diffusion)
2. Adsorption of the gases
3. Reaction on the surface
4. Desorption of the products and
5. Transport of the liberated product from the surface to the bulk gas phase.

Stages 4 and 5 have been dismissed in the case of static fatigue since new crack surface is constantly being exposed as the crack grows leaving behind adsorbed corrosion products on the walls [4]. Desorption and transportation of the liberated products away from the crack tip are therefore not expected to greatly affect the reaction rate.

Of the three remaining processes only chemisorption and chemical reaction at the surface would be expected to depend on both load and relative humidity. In view of this, it was suggested [4] that region I behaviour is due to chemisorption or chemical reaction at the crack tip.

Similarly, only a diffusion-type process would be expected to be stress independent while simultaneously exhibiting a strong concentration dependence. Thus, crack growth in region II has been suggested [4] as being dominated by the rate at which water can be transported to the crack tip.

Region III behaviour is not well understood with a number of workers demonstrating that, in some cases, the position of the curves in that region is dependent on environment [12, 13] and that electrostrictive effects aid crack growth [5].

A later, more quantitative explanation of static fatigue indicated crack velocity in region I was controlled by the chemical potential of the active component in the environment according to [5]

$$V = v_0 a_s \cdot \exp(\mu_{so} + \mu_g + \mu_o)/(RT) \quad (1)$$

where  $v_0$  incorporates terms for frequency factor, transmission and activity coefficients and geometric factors relating to the number of broken bonds;  $a_s$  relates crack velocity dependence to the amount of water in the environment;  $\mu_{so}$ ,  $\mu_g$  and  $\mu_o$  = chemical potential of water in solution, chemical potential of reactive species and chemical potential of activated species respectively. The exponential term therefore contains the crack velocity dependence on stress.  $R$ ,  $T$  = gas constant and temperature respectively.

Increasing the applied load results in an increase in the chemical reaction rate at the crack tip and hence, an increase in crack velocity according to Equation 1. This continues until a situation is reached where the crack velocity is so great that water at the crack tip is used at a rate faster than it can be supplied. At that point crack velocity will depend on how quickly water can be supplied to the crack tip (i.e. diffusion rate) giving rise to region II crack growth behaviour.

Cracks in fibres stressed to the point where crack velocities fall into regions II or III would propagate through a typical 125  $\mu\text{m}$  diameter optical fibre in an extremely short time. In order to ensure such crack growth velocities are not achieved in practice, stringent manufacturing and installation procedures have been adopted for optical fibre cable aimed at keeping the applied fibre stress (and hence, crack growth velocity) confined to region I. It is for this reason that the exact behaviour of glass in region I is of particular significance in determining the lifetime of silica optical fibre. Consequently, subsequent discussion will be restricted to region I behaviour although many aspects are also applicable to the other regions.

At a molecular level, the glass/water interaction has been described by a three step process as illustrated in Fig. 2 [14, 15]:

1. A water molecule from the environment reaches the strained bond at the crack tip and is adsorbed when an oxygen lone pair on the water interacts with a silicon atom either through Van der Waals forces or some covalent bonding. A proton forms a hydrogen bond between the water and the bridging oxygen.
2. Proton transfer to the bridging oxygen atom and electron transfer from the oxygen atom on the water molecule to the silicon atom, occurs simultaneously. This results in the formation of a new Si-O bond and an O-H bond.
3. Rupture of the (assumed) weak remaining hydrogen bond occurs leaving Si-OH groups on the surface of the crack and exposing a new Si-O-Si bond at the crack tip to water.

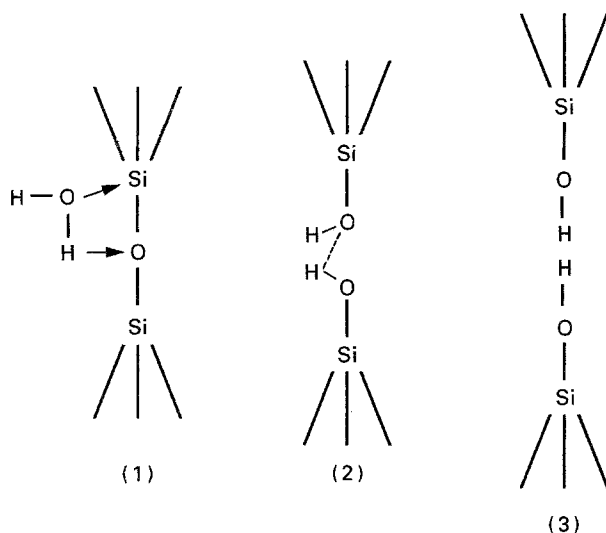


Figure 2 Molecular model of the glass/water interaction. (1) Interaction of a water O-H bond with a glass Si-O bond; (2) Si-O bond and O-H bond formation; (3) rupture of the (assumed) weak O-H bonds (after [14]).

Implicit in this interpretation is the requirement of strained Si-O-Si bonds [16]. Removal of liberated products from the crack tip is not required for the process to continue so supporting the reasoning of earlier workers [4]. Further, the molecular model suggests only those environments having both an electron and proton donor site are capable of inducing static fatigue in a strained glass structure and some evidence for this has been found [17].

The mechanism described above of a reactive species interacting with stressed bonds is currently the most widely accepted explanation of region I behaviour. Other mechanisms have been advanced [18-22], and largely ignored, by researchers in favour of the 3-step model described.

The current view then is that the glass/water interaction requires stressed Si-O bonds in the presence of water. Owing to the extremely low diffusion rate of water through fused silica (diffusion coefficient  $10^{-12}$  to  $10^{-13}$   $\text{cm}^2 \text{s}^{-1}$ , [23]) the process is restricted to the near surface of the glass or to the tips of cracks and defects originating from that surface. The growth rate of cracks responding to this phenomenon then decreases with decreasing stress, decreasing temperature or decreasing humidity. The conditions for static fatigue to occur are almost always achieved at the surface of optical fibres.

### 2.1. Water at the fibre surface

The amount of water needed for static fatigue to occur is exceedingly small with the effect having been found to be significant even in a vacuum of some  $10^{-4}$  Pa [24]. Since it is the partial pressure of water in the medium which is important, static fatigue may be observed even in a liquid which dissolves minute amounts of water ( $< 50$  p.p.m.) [25].

Currently, optical fibres in typical urban cables are encased in a grease-like "filling compound" as well as a number of polymeric layers, partially in an effort to inhibit water ingress to the fibre surface and partially

to protect the fibre from mechanical damage. However, owing to the extremely small amounts of water involved and the ability of the various cable materials to absorb and/or allow water permeation, sufficient water will nearly always be present at the fibre surface to allow static fatigue to occur. It is for this reason that the inert strength of fibres (i.e. the "true" strength without degradation due to static fatigue) is difficult to measure and is usually done at liquid nitrogen temperature, under very high vacuum or by drying and rapidly testing the dry fibres.

Reducing humidity via low temperatures or high vacuum is effective but not practicable to an entire optical network and so the presence of water at the fibre surface must be accepted in ordinary cables. In practice then, minimizing static fatigue in fibres is achieved by minimizing tensile stresses on the fibres and so some attention has been focused on determining the stress below which static fatigue does not occur (i.e. the fatigue limit). If that stress were found to be acceptable from an engineering standpoint, fibres could be installed and manufactured at stresses less than the fatigue limit thereby eliminating the possibility of static fatigue.

A fatigue limit has been observed in soda-lime glass [26] and borosilicate glasses [27, 28] fuelling speculation that such a limit also exists for the high purity fused silica glasses used in the manufacture of optical fibres. The existence of a fatigue limit in those glasses has however, not been definitively established although some authors report evidence suggestive of the fact [16, 29-31]. In the absence of a verified fatigue limit in fused silica glass, a "safe" stress model based on 1% crack growth in 40 years has been advanced [32].

### 2.2. Stress at the fibre surface

Long-term tensile loading of the surface of fibres is commonly thought of as arising as a result of bending of fibre following jointing or repair, cable installation or earth movement following installation. While these are certainly primary sources of fibre tension, fibre drawing conditions such as temperature, drawing force and drawing velocity are also known to greatly influence the mechanical properties of silica fibres. Those factors may result in compressive or tensile "skins" in the outer layer of the fibres [33-38]. Incorrect laying or subsequent earth movement may increase that level of tensile stress, or cancel and overwhelm compressive stresses, resulting in an increase in crack growth velocity and reduced fibre lifetime. Tensile stresses as high as some 72 MPa [39] have been induced in fibres as a result of these effects with those stresses decreasing only negligibly over some 25 years [40].

Stresses are also known to result from fibre coatings. Owing to the different thermal expansion properties of the fibres and their polymeric coatings, optical fibre coatings have been reported as capable of inducing stresses into the fibre surface at both high and low temperatures with such stresses possibly resulting in microbending of the fibre [41-43].

While the macroscopic stress on the surface of the fibre may be small, that stress may be greatly magnified at the tip of flaws in the structure ( $\sigma_c$ ) according to [44]

$$\sigma_c = 2\sigma_a(c/\rho)^{1/2} \quad (2)$$

where  $\rho$  = radius of the tip of the defect. The severity of a defect then is governed by its shape i.e. its depth ( $c$ ) and “sharpness” ( $\rho$ ).

Early production optical fibres suffered from both “extrinsic” and “intrinsic” flaws giving rise to a distribution of fibre strengths as shown in plot (a) of Fig. 3. Extrinsic flaws result from particulate matter such as dust, furnace insulation or impurities in the polymeric coating materials either becoming embedded in the fibre surface or mechanically damaging that surface [45–48]. Intrinsic flaws result from localized material response to mechanical or chemical processing variables and are inherent in virtually all materials at an atomic level. Such flaws cannot, in general, be avoided in a normal production environment. With the instigation of clean-room conditions and other improvements in manufacturing techniques, extrinsic flaws have been virtually eliminated in current production fibre and the severity of intrinsic flaws greatly reduced. Some workers have reported the distribution of fibre tensile strengths to be small and of the order of 5 to  $\approx 6.5$  GPa when drawn and have suggested such fibres are essentially free of extrinsic flaws [49, 50]. Any observed variation in strength has then been attributed to slight fluctuations in fibre diameter during manufacture [50]. With manufacturers currently attempting to minimize diameter fluctuations [51] that range should be further reduced. Production fibres produced today then have a much improved strength distribution over earlier fibres, as shown by plot (b) of Fig. 3.

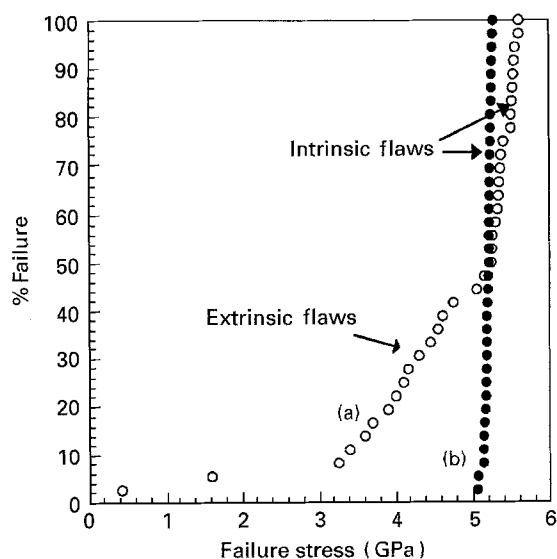


Figure 3 (a) Strength distribution of early optical fibre (O) showing regions of “intrinsic” and “extrinsic” flaw behaviour (after [114]) compared with (b) the purely intrinsic behaviour of more recent production fibre (●) tested in the author’s laboratory. Gauge length and strain rate in both cases were 0.75 m and  $0.5 \text{ min}^{-1}$ , respectively.

Although greatly improved and tending to a single value, the strength of silica fibres is still considerably less than the theoretical strength of fused silica i.e. some 24 GPa [52]. This stems from the presence of the intrinsic flaws which serve to concentrate applied stress giving rise to failure stresses considerably less than the theoretical value. Thus, the tendency towards a single value of fibre tensile strength is a reflection of the tendency towards a single flaw size. Since intrinsic flaws are inherent in real materials, the practical theoretical strength of that material must be its strength when those flaws are taken into account. The theoretical strength of a solid is a value close to one tenth of its elastic modulus ( $E$ ) and so the value for fused silica is of the order of 7 GPa (since  $E \approx 72 \text{ GPa}$ ). This agrees well with the approximately 5 to 6.5 GPa tensile strengths reported for today’s high strength fibres and indicates that current production fibres are approaching their practical theoretical strength and hence, the flaw size is approaching a single, limiting value.

Using the fracture mechanics relationship

$$K_{Ic} = Y\sigma_a c^{3/2} \quad (3)$$

where  $K_{Ic}$  = critical stress intensity factor in pure tensile (mode I) loading ( $0.75 \text{ MPa m}^{1/2}$  for fused silica),  $Y$  = geometric term accounting for, amongst other things, crack shape = 1.26 [53] and  $\sigma_a$  = the applied stress (5–6.5 GPa), the intrinsic flaw depth ( $c$ ) can be calculated to lie in the range 8–14 nm although values as small as approximately 1 nm have been reported [54].

It should be noted that these crack sizes represent idealized “Griffith flaws” [55], that is, the effective length (depth) of an ellipsoidal, “equivalent microcrack” that would cause failure in a piece of fused silica glass with a fracture toughness of  $0.75 \text{ MPa m}^{1/2}$  at the stresses indicated. These “equivalent microcracks” may in no way reflect the true shape of the flaws.

The intrinsic nature of some flaws ensures the fibre surface has regions capable of intensifying even the smallest applied stress making those regions particularly susceptible to static fatigue.

The silica fibres in standard terrestrial cables operating under normal conditions then, undergo static fatigue. This arises since the conditions of stress (either from fibre drawing, cabling, laying or earth movement and magnified by intrinsic flaws) and water (since exceedingly small amounts are required and may permeate through the cable materials to the fibre surface) are nearly always met in practice. Recent work has indicated that the rate of crack growth in fibres is also influenced by:

(a) pH. High pH is known to reduce fibre lifetime and low pH to increase it [56, 57]. pH 12 has been measured in some optical fibre ducts and results from rainwater seeping through overlaying concrete and leaching out alkali ions.

(b) Fibre coating. Poorly adhered coatings reduce fibre lifetime. The degree of coating adherence is determined by glass/coating bonds. Poorly adhered coatings

have fewer glass/coating bonds than well adhered coatings and so have more sites available for the glass/water interaction to occur [58, 59]. Poorly adhered coatings are favoured by some telecommunications organizations since they result in reduced installation and repair times.

(c) Specific ionic species. Lifetime is reduced in the presence of sodium, potassium and calcium ions [60]. Calcium is a major constituent of cement and may be leached out of concrete poured over ducts by rain-water.

Although the phenomenon of static fatigue has been known to occur in silica-based glasses for many years, only recently has work shown that for a more complex system such as an optical fibre, which consists of both silica glass and various polymeric layers, the effect can be influenced by factors other than stress, temperature and humidity.

Various models have been developed to predict the time to failure of fibres subjected to a number of conditions in a variety of environments. None of those models contain terms for pH, ionic species, coating type etc, relying instead on experimental re-evaluation of fibre parameters for the particular test conditions. Despite those shortcomings, such models are used by fibre manufacturers to fulfil the requirements of the various telecommunications authorities world-wide for a guaranteed fibre lifetime, usually specified as some 30 to 40 years, and will be discussed in the next section. The approach adopted here has been phenomenological rather than mathematical since a generalized discussion of shortcomings common to a number of lifetime models is undertaken. A more formalized approach to fibre lifetime modelling may be found in a number of other articles appearing in the literature [29, 53, 61, 62].

### 3. Lifetime modelling

Experimental work on crack growth velocity ( $V$ ) and stress intensity factor ( $K$ , defined in Equation 3) always produced a result similar to Fig. 4 in glass and other brittle materials [6, 7, 63, 64].

From such results it was *empirically* determined that the crack velocity followed a relationship with  $K$  of the form [7]

$$V = A_1 K^n \quad (4a)$$

where  $A_1$  is a constant,  $K$  is the stress intensity factor and  $n$  is the so-called stress corrosion constant, determined by either statically or dynamically loading fibres in the environment of interest (see Section 4.3).

Considerations involving, for example, chemical rate theory and atomistic crack growth models, resulted in a more physically-based relationship of the form of Equation 1 [65, 66] i.e.

$$V = A_2 \exp(A_3 \sigma_a) \quad (4b)$$

where  $A_2$  and  $A_3$  are constants and  $\sigma_a$  is the applied stress. The terms in parentheses usually incorporate both  $n$  and  $K$ , with  $K$  absorbing  $\sigma_a$  as in Equation 3. Many of the lifetime models used today are based on equations having one of these two forms.

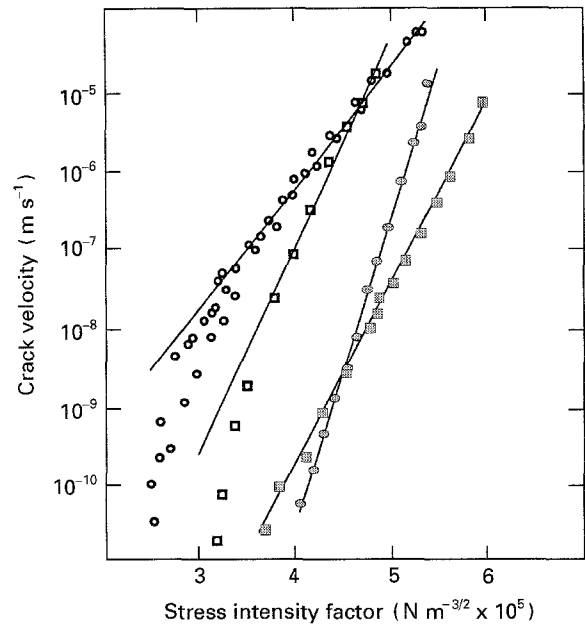


Figure 4 Crack velocity  $V$  versus stress intensity factor  $K$  in region I for a number of glasses (after [81]). Note the deviation from linearity in soda-lime and borosilicate glasses at low stress intensities, indicative of a fatigue limit.  $\circ$  soda-lime;  $\square$  borosilicate;  $\bullet$  silica;  $\blacksquare$  alumino silicate.

Attempts at validating lifetime models for high strength fibres based on Equation 4 have met with mixed success. The general approach has been to assess the fit of experimentally obtained data to those models. Some authors report the equations as satisfactory [29, 67] while others have found some fibres which exhibit behaviour not predicted by models based on those equations [68].

It has been suggested that the power law approach (Equation 4a) is limited in its use owing to its inability to adequately fit the non-linear static or dynamic experimental fatigue data exhibited by some fibres. Accordingly, its usefulness is claimed to be limited to a finite range of stress histories [69]. Further limitations are that the power law approach, unlike the exponential, is not based on any actual physical model, being purely empirical in nature and that lifetime formulae based on it always overestimate lifetime when compared to predictions from other kinetic models [70]. These limitations notwithstanding, the power law approach has been deemed suitable for use in most practical situations [29] and this, combined with its mathematical simplicity, has made it the most commonly used approach for lifetime modelling [71]. However, some authors still favour the exponential dependence of Equation 4b [72, 73] and recent work has indicated the exponential dependence may be more applicable to fibres [74]. Other authors feel that, given the uncertainty in crack growth kinetic models [19] and the error in predictions based on those models (discussed more fully in Section 4.3) a range of models must be considered for lifetime predictions [65].

Regardless of the ultimate form of the lifetime equations based on Equation 4, a number of assumptions were made in order to establish the relationship

presented by that equation, including:

- (i) fibres contained pre-existing flaws that behaved in accordance with fracture mechanics principles both before and at fracture;
- (ii) the extension of those cracks by the glass/water interaction is the primary mechanism governing fibre lifetime;
- (iii) measured parameters such as  $n$  do not change with time for a specific experimental arrangement; and
- (iv) the externally applied stress is the only stress acting on the fibre surface.

Each of these assumptions will now be discussed.

### 3.1. Pre-existing flaws that behave in accordance with fracture mechanics principles

Equation 4 was determined from data obtained from bulk specimens. In such specimens long cracks could be formed and their extension studied under a variety of conditions. Such cracks had a large, sharp front that was well-defined in comparison to microstructural variations in the material and so were amenable to analysis by fracture mechanics principles (e.g. Equations 2 and 3). Extension of that crack front by the mechanism of stress-enhanced environmental corrosion as discussed in Section 2, with its associated lack of desorbed products and no requirement for transportation of liberated products from the crack front, was thus generally accepted as correct.

As discussed in Section 2.2 early production fibres contained not only considerably more extrinsic and intrinsic flaws than do modern fibres, but those flaws were also of greater severity. As a result, early production fibres may have contained true surface cracks which behaved in accordance with the static fatigue model presented in Section 2.0 and so the use of Equation 4 may well have been appropriate.

While there is little doubt that the surface of current production fibres contains some intrinsic defects, calculated to be some 1–14 nm in depth (Section 2.3), the exact nature of many of those defects is unknown. Factors such as localized density variations, non-bridging oxygen atoms, over and under-co-ordinated species, defect centres [75] and the random arrangement of silicon/oxygen tetrahedra leading to “channels” reported to extend more than 1.5 nm into the glass surface [76] may be, or give rise to, intrinsic defects. It has been reported that drawing stresses contribute to the formation of some defect centres which react with water on a local scale [75].

Fibre diameter fluctuations have also been suggested as possible sites for intrinsic defect formation [53]. In general however, owing to the atomic dimensions of many of those defects they may be better described as surface irregularities rather than as true microcracks, although the boundary from surface irregularity to microcrack is ill-defined.

The extremely small size of intrinsic defects in modern optical fibres has made their direct observation difficult and as a result both the “crack” depth ( $c$ ) and “crack” tip radius ( $\rho$ ) of such defects have never been

observed in fibres. Some work has, however, been done on the tip geometry of artificially induced cracks in thin ( $< 1 \mu\text{m}$ ) silica glass films [77]. The true structure of the crack tip of intrinsic defects has been inferred from measurements made at a relatively large distance from the tip and so it is doubtful if their structure is known to a resolution of better than 20 nm. As a result, the extent of the glass/water reaction zone at the crack tip of such defects has not been directly measured but instead, has been estimated to be 1–10 nm depending on the type of glass and the theory used [19].

In the absence of direct measurements, the sharp, well-defined crack front found in bulk specimens was imparted to the nanometre-sized intrinsic defects which were then assumed to behave in the manner of their large counterparts under static fatigue conditions. That is, the overall behaviour of the moving crack front is considered to be unaffected by localized atomic level variations in material density, composition, stress state etc. This continuum approach has been shown to be valid for samples containing cracks of the order of some  $2 \mu\text{m}$  [78] but there is some doubt that on the scale of the calculated equivalent microcrack size in high strength fibres (1–14 nm) the use of a continuum approach, and hence Equation 4, is valid [79, 80]. However, for lack of a better alternative, the continuum model appears to have been widely adopted. It is of interest to note that whereas earlier workers using bulk fused silica specimens reported  $K$  data (as in Fig. 4), current authors investigating the same material but as a fibre, usually report applied stress or simply load thereby avoiding the difficulties associated with fibre flaw shape. There is then some doubt that modern fibres contain pre-existing flaws (microcracks) which do obey the laws of fracture mechanics both before, and at, fracture.

### 3.2. Extension of pre-existing cracks by static fatigue essentially determines lifetime

Some workers suggest that since as-drawn fibres are essentially crack-free and that true cracks propagate rapidly according to Equation 4, the lifetime of today's high strength fibres is governed more by flaw initiation (nucleation) than by crack propagation [17].

It is well established that the dissolution of glass in a suitable medium is stress dependent, occurring more rapidly at higher stress [2, 81]. For that reason it has been suggested that surface flaws can be envisaged as hemispherical pits with dissolution of the glass occurring more rapidly at the bottom of the pit (where stress is highest) than at the top. As a result of the differential dissolution rates the pit becomes both longer and sharper giving rise to increased stress amplification at its tip in accordance with Equation 2 and so a further increase in dissolution rate. When the growth of the depth of the pit becomes sufficiently fast, (slow) dissolution is replaced by (rapid) bond rupture (discussed in Section 2) and the pit depth and shape evolve towards that of a sharp crack. Subsequent growth of that crack is also by bond rupture and eventually leads to failure of the fibre [56]. Recent work on the

effects of ionic species on fibre strength and fatigue has been supportive of this model [60].

An alternative mechanism of crack formation, discussed more fully in the next section, relies on fibre diameter fluctuations as precursor sites [53].

It is not clear then if flaws in fibres represent true cracks or are precursors for such cracks. The method of flaw growth (dissolution or bond rupture) under conditions of static fatigue is also uncertain as is their obedience of the laws of continuum fracture mechanics. At best then, lifetime modelling of modern fibres based on Equation 4 may err only in not incorporating a term for the precursor crack nucleation stage, with the bulk of the fibre lifetime determined by subsequent crack extension according to the mechanism described in Section 2 and obeying the principles of fracture mechanics. At worst however, the bulk of the lifetime may be determined by the precursor stage with its possibly different associated mechanism and the (comparably) rapid propagation stage contributing little to lifetime. In that case, the use of Equation 4 as a basis for lifetime modelling is incorrect.

### 3.3. Measured parameters do not change during a given test

An investigation involving crack stability and kinetic considerations has resulted in the proposition that, when material is removed (by an undisclosed mechanism) from the vicinity of sinusoidal fibre diameter fluctuations a stable crack is formed that will continue to grow. Variations in fibre diameter by themselves are not capable of forming such a crack even if displacement of material in the vicinity is allowed. For the process to continue, an "activation volume" surrounding the crack tip must be involved [53] with that volume governed by local crack tip stresses. It is proposed that  $n$  (the stress corrosion constant) is closely related to the activation volume and, as the shape of the crack tip changes during crack growth, so too does the activation volume and correspondingly, the value of  $n$ . The stress corrosion constant is therefore not considered to be a constant throughout a particular test in that model.

Some support for this may be found in comparing measurements of  $n$  using bulk specimens of fused silica containing through-cracks, with similar tests on fibres. Bulk samples yield values of around  $n = 40$  [82, 83] compared with values of around  $n = 20$  reported for current production fibres [62]. The activation volume for a defect in a fibre would be expected to differ significantly from that for a large through-crack in a bulk specimen, hence explaining the discrepancy in observed  $n$  values [53] between bulk samples of fused silica and fibres.

Changes in the value of  $n$  during testing of optical fibres has also been reported by a number of workers [24, 56, 84, 85] while other authors claim such changes are limited to only certain fibres and environments [29]. Recently, changes in  $n$  during testing have been attributed to the formation of silicic acid through the reaction of the glass with environmental water and

the subsequent etching of the fibre surface giving rise to pits which act as defects [70].

### 3.4. Externally applied stress is the only stress acting at the fibre surface

As discussed in Section 2.2, the applied tensile stress may not be the only stress acting on the fibre surface. Residual surface stresses from fibre manufacturing can be high and may result in either an over-estimation of the apparent applied tensile stress if that residual stress is compressive, or an under-estimation if it is tensile.

Fig. 5 shows the effect of residual stress on the stress corrosion constant ( $n$ ) for a production, single mode, u.v.-cured acrylate coated, silica optical fibre. In excess of 25 fibres were tested in 2-point bend [86] at each of three faceplate velocities by the author. Open circles represent values of  $\log_e$  of the (Weibull) median stress of the load-at-failure data as determined by the 2-point bend equipment at each velocity (uncorrected data). Closed circles represent that same data corrected for a residual tensile stress of 70 MPa (=0.969 microstrain). The correction was obtained by adding  $0.969 \mu\epsilon$  to the strain value as determined by the 2-point facility from the faceplate separation at failure ( $\epsilon$ ). That strain was then used to determine the strain-at-failure according to [87]

$$E = E_0[1 + 3.2(\epsilon) + 8.48(\epsilon^2)] \quad (5)$$

where the term in parentheses represent first and second order corrections to the elastic modulus according to the applied strain and  $E_0$  = Young's modulus at zero strain (72.2 GPa for pure silica). Failure stress was then calculated in the standard manner.

As can be seen from Fig. 5, the incorporation of the residual tensile stress has reduced the value of the

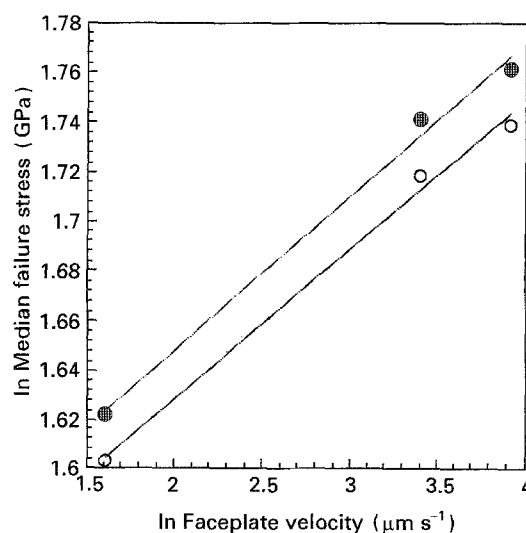


Figure 5 Effect of a 70 MPa tensile residual stress on the stress corrosion constant  $n$  for a production, single mode, u.v.-cured acrylate coated, silica optical fibre. In excess of 25 fibres were tested in 2-point bend at each of the three faceplate velocities. Median values were obtained using the maximum likelihood method of Thoman *et al.* [104].  $\circ$  uncorrected data  $n = 17.56$ ;  $\bullet$  corrected data  $n = 17.05$ .

stress corrosion constant from  $n = 17.56$  (uncorrected) to  $n = 17.05$  (corrected).

Taking the lifetime model proposed by Evans & Wiederhorn as an example [88]

$$t_f = BS_i^{n-2}\sigma_a^{-n} \quad (6)$$

and using  $B = 1.3 \times 10^{-8} \text{ GPa}^2 \text{ s}$  and  $S_i = 12.2 \text{ GPa}$  as representative values for a u.v.-cured acrylate coated, single mode silica optical fibre [89] and taking  $\sigma_a = 27 \text{ MPa}$  as a reasonable installation stress, gives

$$t_f \approx 36.6 \times 10^{35} \text{ s for } n = 17.56 \quad (7)$$

and

$$t_f \approx 1.6 \times 10^{35} \text{ s for } n = 17.05 \quad (8)$$

a reduction in predicted lifetime of some 22 times.

As can be seen, ignoring residual stresses affects the measurement of  $n$  only marginally but can lead to significant variations in predicted lifetime.

Even in fibres having no macro-residual stresses, localized residual stresses may form on a micro-scale along the fibre surface as a result of either mechanical or chemical interaction of the preform/fibre surface with a gas or solid impurity. Such interactions may not generate sufficient stress to nucleate a crack and so leave the affected region in a state of localized stress [49]. Considerable scatter in time-to-failure data would therefore be expected from such fibres.

It appears then that many of the fundamental issues related to understanding the true nature of the glass/water interaction in current production fibres are currently somewhat contentious. There is little evidence to suggest flaws in these fibres obey the principles of continuum fracture mechanics or even that the growth of such flaws is the dominant mechanism governing fibre lifetime. Three other issues have further added to the confusion surrounding lifetime modelling: flaw distribution, the nature of the crack tip and the techniques used to obtain and analyse data from fibres for use in lifetime models, and these will be the focus of the next section.

## 4. Other issues

### 4.1. Flaw distribution

The above discussion has been based on findings which suggest current production fibres have a narrow (essentially single valued) flaw size. Such findings result from tests on lengths of fibre ranging from microns to a number of metres. However, there is some evidence to indicate the flaw distribution determined from tests on such short fibre lengths is not truly indicative of the distribution found in a multi-kilometre network. It has been demonstrated that large flaws (of the order of 1 to 3  $\mu\text{m}$ ) exist in multi-kilometre fibre lengths but are not common [90]. As a result, short sections of fibre are unlikely to contain those flaws and so results based on short length tests are likely to give an erroneous view of the true flaw distribution. It has further been suggested that it is the fatigue behaviour of those large flaws which is primarily responsible for the lifetime of current production optical fibres [91]. Other authors feel that both short

(0.6 m) length tests and long length (kilometre) proof-tests formed a single distribution [92] and, provided that data was collinear, could be used for lifetime calculations [29].

### 4.2. The nature of the crack tip

Recent work has raised the possibility that the shape of the crack tip plays a vital role in its environmental fatigue behaviour. That work was based on surface force considerations by Barenblatt [93] which suggested a crack tip under finite stress is cusp-shaped (Fig. 6(b)) owing to interactions between atoms on either side of the crack at its tip, rather than ellipsoidal as proposed by Griffith (Fig. 6(a)) and as usually assumed in lifetime models. As well as the exact position of the crack tip therefore being ill-defined, the further implications of this work are that at low stress, water molecules are simply too big to reach the crack tip, becoming trapped some distance from the tip by the interaction of crack wall surface forces [21]. Water molecules then reach the tip by diffusion through the surrounding material [20], a process requiring a significant amount of time owing to the low diffusion rate of water through silica glass. At higher stresses, the shape of the tip tends more towards that proposed by Griffith [55] and water molecules can reach the tip

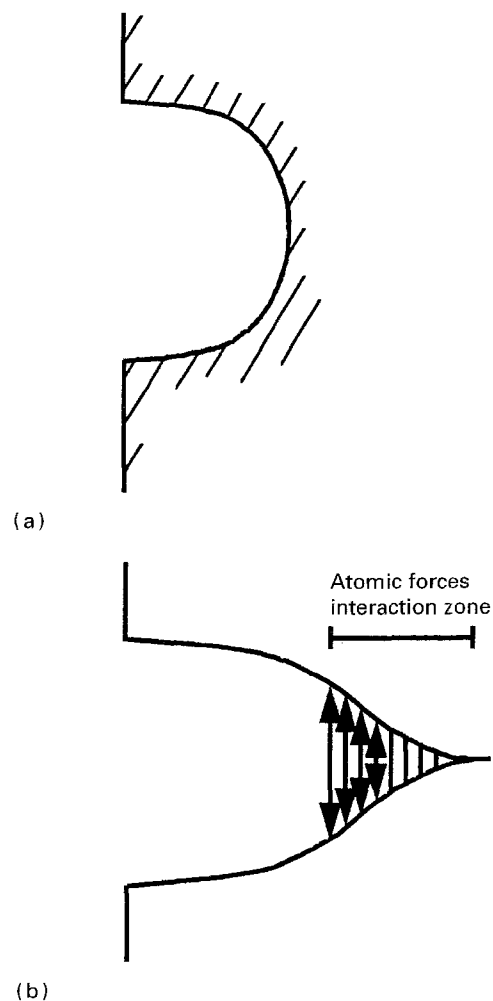


Figure 6 Comparison of (a) Griffith and (b) Barenblatt crack profiles (after [93]).



unhindered, presumably extending the crack in the manner described in Section 2. Thus, this model proposes a diffusion stage prior to crack extension by bond rupture, in contrast to one of the models proposed in Section 3.2 which suggested a dissolution stage prior to crack extension by bond rupture. It is of interest to note that, while some workers report an increase in strength of cracked samples left in air or heated in water (attributed to blunting of the crack tip by static fatigue [94]), other workers have reported no such increase in strength and attribute that to the inability of water to reach the crack tip, thereby supporting the above model [20].

The use of Equation 4 as a basis for lifetime modelling makes the implicit assumption that the crack tip radius ( $\rho$ ) remains constant throughout the crack growth process and that changes in the stress intensity factor ( $K$ ) result only from changes in applied load and crack length ( $\sigma_a$  and  $c$  respectively, in Equation 3). Thermodynamic considerations of the fracture process have, however, been used to suggest that a minimum tip radius equal to approximately 10 interatomic spacings must be achieved for fracture to occur. For smaller radii cracks subjected to a tensile stress, crack tip atoms rearrange themselves to achieve that minimum radius [95]. That is, the shape of the crack tip may change with load, alternating between “blunt” ( $\rho > 10$  interatomic spacings) and “sharp” ( $\rho < 10$  interatomic spacings) as crack extension continues.

The suggestion that the shape of the crack tip does not remain constant throughout the static fatigue process has been supported by a study of abraded high-silica glass rods immersed in hot water. That work indicated that sharp crack tips could become blunted by a dissolution and reprecipitation process necessitating the formation of a sharp crack before crack extension by bond rupture could commence at low loads. It was further postulated that the formation of such a crack could take a longer time than its growth to a critical length by the bond rupture mechanism [96].

In Section 2.2 it was noted that the assumed shape of the equivalent microcrack may bear no real resemblance to the actual shape of the flaw in the material. The true flaw shape will affect both  $c$  and  $Y$  in Equation 3 and hence,  $K$  in Equation 4. The preceding discussions, in conjunction with the “dissolution” model of Section 3.2 and the “activation volume” model of Section 3.3, indicate that the crack tip processes are not well understood and that assumptions concerning the direct ingress of water to the crack tip, and the unchanging shape of that tip, may not be valid. The shape of the flaws in silica optical fibres may well change as the static fatigue process begins and progresses so affecting the actual mechanism of fatigue [78]. Differences in fatigue behaviour between intrinsic and extrinsic flaws might therefore be expected and have indeed been reported [91, 97].

The discrepancy in the stress corrosion constant for bulk silica glass and silica fibre mentioned in Section 3.3 may be a further manifestation of the crack tip/fatigue mechanism interaction. If this is in-

deed found to be the case, the relationship between crack velocity ( $V$ ) and  $K$  could assume values which no longer give rise to equations of the form of Equation 4 for all stages in the static fatigue process.

While the model of crack extension suggested by Michalske and Freiman (Section 2) is generally accepted as correct for stress enhanced environmental crack growth in glass, the size and shape of flaws to which it is applicable in that material is somewhat contentious. Indications are that a precursor stage exists in which the crack forms and/or grows (by some mechanism) to a critical size/shape which is then conducive to the Michalske–Freiman model. It has been suggested that this precursor stage contributes significantly to fibre lifetime and appears to have been ignored in current lifetime models.

### 4.3. Fibre data acquisition and analysis

Lifetime models presented in the literature are based on obtaining certain fibre parameters with one of the most common being the stress corrosion constant ( $n$ ). Many proposed lifetime models are heavily dependent on  $n$  since that value is often the power to which some terms in the lifetime equation are raised (e.g. Equation 4(a)). For that reason the bulk of the following discussion will be restricted to  $n$  although many aspects are also applicable to other fibre parameters required for use in lifetime models. There are essentially two approaches for determining the stress corrosion constant, the dynamic approach and the static approach.

Since the mechanism of static fatigue is thought to involve water at the crack tip, it might be expected that for a fibre loaded slowly, water has more time to interact with the glass. As a consequence cracks in such a fibre are likely to extend resulting in a reduced fibre failure load when compared with the same fibre loaded at a faster rate. This is observed in practice and forms the basis of the dynamic method of determining the stress corrosion constant.

In the dynamic method, a number of fibres undergo tensile loading to failure at a number of different loading rates and the failure loads noted. A 2-parameter Weibull probability density function [98] is then fitted to that data from which the median (for example) failure stress (probability of failure = 0.5) for each rate is obtained [29]. A plot of  $\log_e$  (median failure stress) against  $\log_e$  (applied stress rate) is then constructed and the line of best fit to that data determined. The (dynamic) stress corrosion constant is then obtained from the slope of that line [62].

The static method involves loading lengths of fibre to a particular stress and determining the time-to-failure of those fibres. Since static fatigue is known to involve both water *and* stress, the higher the load (stress) the shorter is the expected time-to-failure. Data can be obtained in a number of ways including, for example, winding a number of fibres around a mandrel of known radius [86], dead-weight loading or by bending fibres to a known radius using a special fixture [29]. The time and date of failure of all fibres tested at each stress are recorded and that time-to-failure data fitted to a 2-parameter Weibull

probability density function from which the median (for example) time-to-failure at each stress is obtained. A plot of  $\log_e$  (median time-to-failure) against  $\log_e$  (applied stress) is then constructed and the line of best fit to that data determined. The stress corrosion constant is the negative slope of that line.

Regardless of the technique used for determining the stress corrosion constant, statistical analysis of the experimental data is required. Although a number of approaches have been suggested [99, 100] the most widely adopted method of analysis has been to apply Weibull statistics to obtain the median (or alternatively, the mean) value of the data as described above [29, 62]. However, some authors suggest the use of the mean or median value leads to large uncertainties in fatigue parameters owing to the inefficient use of the data [100]. Others feel that there are no theoretical considerations favouring the use of the Weibull distribution over the normal distribution [101], with its widespread use being attributable to mathematical convenience [95].

The use of the 2-parameter Weibull distribution necessitates the evaluation of the Weibull shape ( $m$ ) and the scale ( $\lambda$ ) parameters. As with any statistical approach to data analysis a prime requirement is that a sufficient number of samples be tested to ensure a suitably accurate result. In the case of the 2-parameter Weibull distribution, the accuracy in  $m$  increases with sample size tested and it has been shown that  $m$  is within 10% of the true value for a sample size in excess of approximately 30 [102]. The accuracy in  $\lambda$  is dependent on both the sample size tested and the accuracy in  $m$  [103]. A number of techniques exist for evaluating  $m$  and  $\lambda$  [104, 105] and these techniques yield values of differing accuracy [106, 107]. Further, the accuracy in determining  $\lambda$ ,  $n$  and other lifetime constants depends, for both static and dynamic methods, in a complex and interrelated manner on  $m$ ,  $n$ , number of samples tested and the range of stresses applied and, for dynamic tests, also on the number of stressing rates used [105, 108]. Some variation in the calculated values of the Weibull parameters and the stress corrosion constant is therefore inevitable, resulting in an unavoidable variation in predicted lifetime.

It has been suggested that estimates for the uncertainty in minimum lifetime predictions can be made provided the coefficient of variation of the experimentally derived parameters (including  $n$ ) is less than approximately 10% [109] and the statistical reproducibility of parameters such as  $n$  is known as a function of sample size [108]. Analyses for determining the statistical reproducibility of  $n$  and the uncertainty in lifetime predictions have been presented [105, 109, 110]. Those analyses used linear regression to fit data and the finding that the Weibull parameters were normally distributed. They also relied on the law of propagation of errors [108].

Recent work indicates that maximum likelihood methods are more accurate in obtaining Weibull parameters than linear regression and that those parameters follow an asymmetric, slightly skewed distribution [107]. Further, the law of propagation of errors approach is thought to be unsuitable for fibres having

a broad strength distribution and small slope, such as hermetically jacketed fibres [111].

As a consequence of the complex interdependence of the various statistical and lifetime parameters, combined with uncertainty in the most appropriate methods for obtaining data (static or dynamic) and of analysing that data once obtained, there is currently no universally accepted method for determining the lifetime of silica optical fibres. Some local standards have, however, been advanced [112].

Dynamic and static approaches have their advantages and limitations [62]. Dynamic tests are carried out in seconds or hours in ambient or inert environments and allow for the relatively quick accumulation of data. Static testing, by contrast, is usually carried out over longer periods (days to years), often in a hostile environment. Both static and dynamic testing can be undertaken on long lengths of fibre with the trend today being towards dynamically testing fibre in 2-point bend [86, 89]. This technique samples a section of the fibre surface equivalent to a length under pure tensile loading of some 10 to 1000  $\mu\text{m}$  [86] whereas static testing involving mandrel bending or dead weight loading allows considerably more, or all, of the fibre surface to be sampled. It is therefore more likely to encounter a large flaw of the type discussed in Section 4.1 which may well allow ready access of water to the crack tip and behave in accordance with the principles of fracture mechanics. Typically however, in excess of 20 fibres ranging in length from a few centimetres to some tens of metres, are tested at each loading rate or at each applied stress and so the likelihood of encountering more than one of those large flaws is not high. As a consequence, the presence of such a flaw is likely to have only a minimal effect on the (median) value determined from the Weibull function. Although minimal, this raises the possibility that the test method employed has a bearing on the value of the stress corrosion constant.

While both forms of testing should, in principle, yield the same value for  $n$  for the same environment the literature indicates some confusion on this point. Some authors report little difference, either by averaging published data over a range of fibres [30, 95] e.g. average dynamic = 22.4 and average static = 22.1 [30] or by comparing results from the same fibre e.g. dynamic = 15.9 while static = 14.3 [67]. While other workers claim substantial differences when comparing results from the same fibre e.g. dynamic = 17.0, static = 37.6 [113].

As illustrated in Section 3.4 and by other workers [62], even small variations in  $n$  can lead to large variations in calculated lifetime. Thus, while *numerical* differences in the stress corrosion constant obtained using static or dynamic techniques may be small, the *practical* significance of such variations to lifetime predictions is immense. It is therefore essential that experimentally determined parameters for lifetime predictions be as accurate as possible and that a standard technique for obtaining them be developed. Currently, no such method has been accepted by the general scientific community or adopted internationally.

## 5. Conclusions

Certain facts are known about the stress enhanced environmental corrosion of silica optical fibres. They are known to exhibit reduced strength when stressed in the presence of water, liquids of high pH and certain ions and the rate of that degradation is known to increase as temperature increases in the range to about 90 °C. On these facts most researchers agree. On many of the fundamental issues related to these facts however, there is little agreement.

A basic model for the environmental fatigue process in glass has been advanced, based on preferred rupture of stressed bonds in the presence of water and is widely accepted as correct for bulk glass. An expression based on experimental work on bulk glass has been for-

mulated and forms the basis of many current lifetime models. Both the mechanism of environmental fatigue and the expression have been assumed to apply to the more complex, flaw-free silica glass/polymeric coating systems found in optical fibres. This assumption is now being questioned in light of work on crack shape and crack-tip forces.

Other processes which act as precursors to crack extension by bond rupture are now being proposed and have been suggested as playing a greater part in determining the lifetime of current production fibres than crack extension by bond rupture. Similarly, evidence exists to indicate that various assumptions involving the fracture mechanics framework on which current lifetime theory is built – originally adopted for

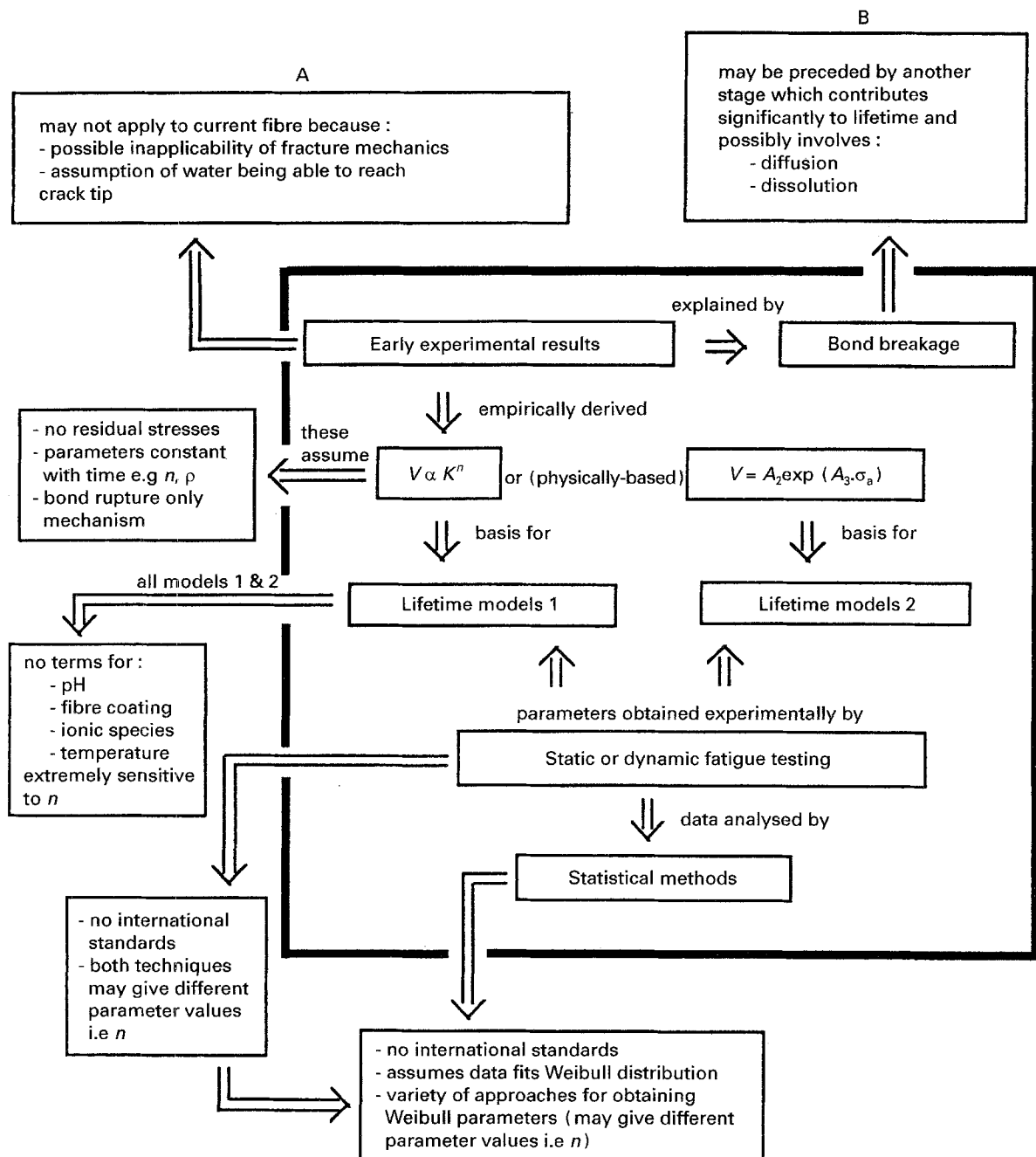


Figure 7 Summary of the current state of fibre lifetime work. The heavily outlined box represents the generally accepted approaches to fibre lifetime modelling. Boxes A and B above this indicate recent findings which cast some doubt on the applicability of early experimental work to current fibres (A) as well as the existence of the bond rupture mechanism as the primary contributor to fibre lifetime (B). Remaining boxes indicate shortcomings at various points in the current approaches. Note that none of these shortcomings or recent findings are usually addressed within the realm of current approaches.  $V$  = crack growth rate (velocity),  $K$  = stress intensity factor,  $n$  = stress corrosion constant,  $A_2$  and  $A_3$  are constants and  $\sigma$  = applied stress.

analysis involving large cracks in bulk samples – may not be applicable to the nanometre-sized intrinsic surface irregularities found in current fibre.

It is suggested that the early model is applicable to the relatively large, abundant, well-defined extrinsic flaws found in early production fibres and to the occasional large flaw found in long lengths of current production fibre, but is no longer applicable to the bulk of that fibre. Instead, the literature indicates that a two-stage model consisting of a precursor non-continuum stage possibly involving diffusion/and or dissolution processes, followed by the bond rupture/continuum fracture mechanics approach may be more suited to the small, ill-defined, abundant intrinsic flaws found in current production fibre.

Controversy also arises in the fundamental form of current lifetime models with some authors preferring the power law model while others support the exponential law approach. The methods used in obtaining various fibre lifetime parameters – such as the stress corrosion constant ( $n$ ) – for use in those equations are also contentious with issues such as test technique (static or dynamic), the use of the 2-parameter Weibull distribution and the accuracy in analysis techniques (and hence fibre lifetime parameters) also being questioned. These factors lead to an uncertainty in calculated lifetime parameters (such as  $n$ ) and that uncertainty, combined with the extreme sensitivity of many lifetime equations to those parameters, casts some doubt on the usefulness of such equations to any but those fibres exhibiting exceptional longevity. The error in predicted lifetime for other fibres could be more than their calculated lifetime. This raises the possibility of over-engineered fibres with their associated higher costs. More fundamental concerns of the constancy, relevance and interpretation of lifetime parameters have also been raised. As a consequence, there are currently no internationally accepted standards for determining the stress corrosion constant or any other fibre lifetime parameters, although some local standards have been advanced [112].

These issues are summarised in Fig. 7, which represents the current state of fibre lifetime work.

It is not surprising then that fibre lifetime modelling is presently in a state of flux, as evidenced by the more than 15 different lifetime equations appearing in the literature [e.g. 53, 65, 71, 72, 73]. Much effort is being expended world-wide to resolve many of the issues raised here and to develop a standard, reliable method of accurately predicting the lifetime of silica fibres in a real network. Currently however, no such method exists and so estimates of fibre lifetime based on the present state of knowledge and existing models must be viewed with scepticism.

### Acknowledgements

The author gratefully acknowledges the assistance provided by the staff of the National Information Resource Centre in the preparation of this work with special thanks to Janet Lindner for her tolerant, positive and extremely helpful manner.

### References

1. L. GRENET, *Bull. Soc. Encour. Industr. Nat. Paris* **4** (1899) 838.
2. R. J. CHARLES, *J. Appl. Phys.* **29** (1958) 1549.
3. *Idem.*, *ibid.* **29** (1958) 1554.
4. S. M. WIEDERHORN, *J. Amer. Ceram. Soc.* **50** (1967) 407.
5. S. M. WIEDERHORN, S. W. FREIMAN, E. R. FULLER and C. J. SIMMONS, *J. Mater. Sci.* **17** (1982) 3460.
6. S. M. WIEDERHORN, *Int. J. Fracture Mechanics*, **4** (1968) 171.
7. A. G. EVANS, *J. Mater. Sci.* **7** (1972) 1137.
8. M. MATSUI, T. SOMA and I. ODA, in "Fracture mechanics of ceramics". Vol. 4. Edited by R. C. Bradt, D. P. H. Hasselman and F. F. Lange (Plenum Press, New York, 1978).
9. T. C. BAKER and F. W. PRESTON, *J. Appl. Phys.* **17** (1946) 170.
10. R. J. CHARLES and W. B. HILLIG in Symposium on Mechanical Strength of Glass and Ways of Improving It, Florence, Italy, September (1961) p. 511.
11. S. GLASSTONE, K. J. LAIDLER and H. EYRING, "The theory of rate processes" (McGraw-Hill, New York, 1941).
12. S. W. FREIMAN, *J. Amer. Ceram. Soc.* **57** (1974) 350.
13. H. RICHTER, "The physics of non-crystalline solids" (Tech. Publications, Aedermannsdorf, Switzerland, 1977).
14. T. A. MICHALSKE and S. W. FREIMAN, *Nature* **295** (1982) 511.
15. T. A. MICHALSKE and G. A. FISK, *J. Appl. Phys.* **58** (1985) 2736.
16. T. A. MICHALSKE and B. C. BUNKER, *ibid.* **56** (1984) 2686.
17. K. HIRAO and M. TOMOZAWA, *J. Amer. Ceram. Soc.* **70** (1987) 377.
18. D. MAUGIS, *J. Mater. Sci.* **20** (1985) 3041.
19. S. M. WIEDERHORN, in "Fracture mechanics of ceramics". Vol. 4. Edited by R. C. Bradt, D. P. H. Hasselman and F. F. Lange (Plenum Press, New York, 1978).
20. B. R. LAWN, D. H. ROACH and R. M. THOMSON, *J. Mater. Sci.* **22** (1987) 4036.
21. B. R. LAWN and S. LATHABAI, *Materials Forum* **11** (1988) 313.
22. J. A. GREENWOOD and K. L. JOHNSON, *Phil. Mag.* **A43** (1981) 697.
23. K. KOKURA, M. TOMOZAWA and R. K. MacCRONE, *J. Non-Cryst. Solids* **111** (1989) 269.
24. W. J. DUNCAN, P. W. FRANZ and S. P. CRAIG, in "Strength of inorganic glass", edited by C. R. Kurkjian (Plenum Press, New York, 1985).
25. S. W. FREIMAN, in "Strength of inorganic glass", edited by C. R. Kurkjian (Plenum Press, New York, 1985).
26. T. A. MICHALSKE, in "Fracture mechanics of ceramics". Vol. 5. Edited by R. C. Bradt, A. G. Evans, D. P. H. Hasselman and F. F. Lange (Plenum Press, New York, 1983).
27. S. M. WIEDERHORN and H. JOHNSON, *J. Amer. Ceram. Soc.* **56** (1973) 192.
28. C. J. SIMMONS and S. W. FREIMAN, *J. Non-Cryst. Solids* **38-39** (1980) 503.
29. D. R. ROBERTS, E. CUELLAR, M. T. KENNEDY, M. T. et al., *Optical Eng.* **30** (1991) 716.
30. R. D. MAURER, in "Strength of inorganic glass", edited by C. R. Kurkjian (Plenum Press, New York, 1985).
31. K. T. WAN, S. LATHABAI and B. R. LAWN, *J. Europ. Ceram. Soc.* **6** (1990) 259.
32. G. S. GLAESEMANN and S. T. GULATI, *Optical Eng.* **30** (1991) 709.
33. U. C. PAEK and C. R. KURKJIAN, *J. Amer. Ceram. Soc.* **58** (1975) 330.
34. H. SCHONHORN, H. N. VAZIRANI and H. L. FRISCH, *J. Appl. Phys.* **49** (1978) 3703.
35. P. S. OH, J. J. McALARNEY and D. K. NATH, *J. Amer. Ceram. Soc. (Comm.)* **65** (1983) C84.
36. P. C. P. BOUTEN, W. HERMANN, C. M. G. JOCHEM and D. U. WIECHERT, *J. Lightwave Technol.* **7** (1989) 555.
37. P. K. BACHMANN, W. HERMANN, H. WEHR and D. U. WIECHERT, *Appl. Optics* **25** (1986) 1093.
38. *Idem.*, *ibid.* **26** (1987) 1175.
39. C. R. KURKJIAN and U. C. PAEK, *J. Amer. Ceram. Soc.* **61** (1978) 176.

40. Y. MOHANNA, J-M. SAUGRAIN, J-C. ROUSSEAU and P. LEDOUX, *J. Lightwave Tech.* **8** (1990) 1799.
41. E. HANSON, *Fiber Integrated Optics* **3** (1980) 113.
42. T. A. LENAHER, *AT&T J.* **64** (1985) 1565.
43. E. SUHIR, *Polymer Eng. Sci.* **30** (1990) 108.
44. C. E. INGLIS, *Trans. Inst. Naval Archit.* **55** (1913) 219.
45. R. D. MAURER, *J. Non-Cryst. Solids* **42** (1980) 197.
46. F. A. DONAGHY and D. R. NICOL, *J. Amer. Ceram. Soc.* **66** (1983) 601.
47. R. G. HUFF and F. V. DIMARCELLO, *J. Lightwave Technol.* **LT-3** (1985) 950.
48. D. P. JABLONOWSKI, U. C. PAEK and L. S. WATKINS, *AT&T Tech. J.* **66** (1987) 33.
49. F. V. DIMARCELLO, C. R. KURKJIAN and J. C. WILLIAMS, in "Optical fiber communications. Vol. 1. Fibre fabrication" edited by Tingye Li (Academic Press, Orlando, Florida, 1985).
50. C. R. KURKJIAN and U. C. PAEK, *Appl. Phys. Lett.* **42** (1983) 251.
51. E. D. JUNGBLUTH, *Laser Focus World July* (1992) 20.
52. N. P. BANSAL and R. H. DOREMUS, in "Handbook of glass properties" (Academic Press, Orlando, Florida, 1986) Chapter 12.
53. P. C. P. BOUTEN and G. De WITH, *J. Appl. Phys.* **64** (1988) 3890.
54. C. R. KURKJIAN and J. T. KRAUSE, in "Stress Corrosion Workshop" (National Bureau for Standards, 1982).
55. A. A. GRIFFITH, *Proc. Roy. Soc. London Phil. Trans., Series A* **221** (1921) 163.
56. M. J. MATTHEWSON and C. R. KURKJIAN, *J. Amer. Ceram. Soc.* **71** (1988) 177.
57. J. T. KRAUSE and C. J. SHUTE, *Advanced Ceram. Mater.* **3** (1988) 118.
58. T. WEI and B. J. SKUTNIK, *J. Non-Cryst. Solids* **102** (1988) 100.
59. B. J. SKUTNIK, B. D. MUNSEY and C. T. BRUCKER, *Proc. Mater. Res. Soc. Symp.* **88** (1987) 27.
60. V. V. RONDINELLA and M. J. MATTHEWSON, *SPIE* **1366**, "Fiber optics reliability: benign and adverse environments IV (1990) p. 77.
61. Y. MITSUNAGA, Y. KATSUYAMA and Y. ISHIDA, *Electron. Lett.* **17** (1981) 567.
62. F. P. KAPRON and H. H. YUCE, *Optical Eng.* **30** (1991) 700.
63. P. W. R. BEAUMONT and R. J. YOUNG, *J. Mater. Sci.* **10** (1975) 1334.
64. B. J. PLETKA and S. M. WIEDERHORN, *ibid.* **17** (1982) 1247.
65. M. J. MATTHEWSON, *SPIE* **1580** "Fiber Optic Components and Reliability" (1991) p. 130.
66. T. A. MICHALSKE and S. W. FREIMAN, *J. Amer. Ceram. Soc.* **66** (1983) 284.
67. D. KALISH and B. K. TARIYAL, *ibid.* **61** (1978) 518.
68. W. J. DUNCAN, *ibid.* **69** (1986) C132.
69. K. ABE, G. S. GLAESEMANN, S. T. GULATI and T. A. HANSON, *Optical Eng.* **30** (1991) 728.
70. M. J. MATTHEWSON and V. V. RONDINELLA, *SPIE* **1791** "Optical materials reliability and testing" (1992) p. 51.
71. W. W. GRIFFIOEN, T. BREULS, G. COCITO et al., *SPIE* **1791** "Optical materials reliability and testing" (1992) p. 190.
72. R. H. DOREMUS, in "Strength of inorganic glass", edited by C. R. Kurkjian (Plenum Press, New York, 1985).
73. S. TANAKA, Y. KAMEO, O. ICHIKAWA et al., *Sumitomo Electric. Technical Rev.* **21** (1982) 47.
74. D. INNIS, C. R. KURKJIAN and D. L. BROWNLOW, *J. Amer. Ceram. Soc.* **75** (1992) 3485.
75. Y. HIBINO and H. HANAFUSA, *J. Appl. Phys.* **61** (1987) 1806.
76. S. H. GAROFALINI, in Proceedings of the Second International Conference on Effects of Modes of Formation on the Structure of Glasses. Vanderbilt University, Nashville, TN, USA, June (1987) p. 21.
77. Y. BANDO, S. ITO and M. TOMOZAWA, *J. Amer. Ceram. Soc. (Comm.)* **67** (1984) C-36.
78. T. P. DABBS, B. R. LAWN and P. L. KELLY, *Phys. Chem. of Glasses* **23** (1982) 58.
79. P. K. GUPTA, in "Strength of inorganic glass" edited by C. R. Kurkjian (Plenum Press, New York, 1985).
80. T. P. DABBS and B. R. LAWN, *J. Amer. Ceram. Soc.* **68** (1985) 563.
81. W. B. HILLIG and R. J. CHARLES, in "High strength materials", edited by V. F. Zackey (Wiley & Sons, New York, 1965).
82. S. M. WIEDERHORN and L. H. BOLZ, *J. Amer. Ceram. Soc.* **53** (1970) 543.
83. J. E. RITTER and C. L. SHERBURNE, *J. Amer. Ceram. Soc.* **54** (1971) 601.
84. T. T. WANG and H. M. ZUPKO, *J. Mater. Sci.* **13** (1978) 2241.
85. H. C. CHANDAN and D. KALISH, *J. Amer. Ceram. Soc.* **63** (1982) 171.
86. M. J. MATTHEWSON and C. R. KURKJIAN, *ibid.* **70** (1987) 662.
87. J. T. KRAUSE, L. R. TESTARDI and R. N. THURSTON, *Phys. Chem. Glasses* **20** (1979) 135.
88. A. G. EVANS and S. M. WIEDERHORN, *Int. J. Fracture* **10** (1974) 379.
89. W. GRIFFIOEN, G. SEGERS and E. Van LOENEN, in Proceedings of the Thirty-ninth International Wire and Cable Symposium, November, Reno, NV, USA (1990) p. 368.
90. S. T. GULATI, J. D. HELFINSTINE, G. S. GLAESEMANN et al., *SPIE* **842** "Fiber optics reliability: benign and adverse environments" (1988) p. 22.
91. S. T. GULATI, *Photonics Spectra* **26** (1992) 78.
92. R. D. MAURER, *Appl. Phys. (Lett.)* **27** (1975) 220.
93. G. I. BARENBLATT, *Adv. Appl. Mech.* **7** (1962) 55.
94. S. ITO and M. TOMOZAWA, *J. Amer. Ceram. Soc.* **65** (1982) 368.
95. R. H. DOREMUS, in "Strength of inorganic glass", edited by C. R. Kurkjian (Plenum Press, New York, 1985).
96. M. TOMOZAWA and K. HIRAO, *J. Non-Cryst. Solids* **95-96** (1987) 149.
97. J. D. HELFINSTINE, *J. Amer. Ceram. Soc. (Disc. and Notes)* **63** (1980) 113.
98. W. WEIBULL, *J. Appl. Mech.* **18** (1951) 293.
99. J. E. RITTER (Jr) in "Fracture mechanics of ceramics", Vol. 4. Edited by R. C. Bradt, D. P. H. Hasselman and F. F. Lange (Plenum Press, New York, 1978).
100. K. JAKUS, D. C. and J. E. RITTER, *J. Mater. Sci.* **3** (1978) 2071.
101. R. H. DOREMUS, *J. Appl. Phys.* **54** (1983) 193.
102. J. D. SULLIVAN and P. H. LAUZON, *J. Mater. Sci. (Lett.)* **5** (1986) 1245.
103. G. QUINN, *J. Amer. Ceram. Soc.* **73** (1990) 2374.
104. D. R. THOMAN, L. J. BAIN and C. E. ANTLE, *Technometrics* **11** (1969) 445.
105. J. E. RITTER (Jr), N. BANDYOPADHYAY and K. JAKUS, *J. Amer. Ceram. Soc. (Disc. and Notes)* **62** (1979) 542.
106. J. M. G. LEONARDUS, D. de WITH and G. de WITH, *J. Amer. Ceram. Soc.* **74** (1991) 2293.
107. R. LANGLIOIS, *J. Mater. Sci. (Lett.)* **10** (1991) 1049.
108. J. E. RITTER (Jr), N. BANDYOPADHYAY and K. JAKUS, *Ceram. Bull.* **60** (1981) 798.
109. D. F. JACOBS and J. E. RITTER, *J. Amer. Ceram. Soc.* **59** (1976) 481.
110. S. M. WIEDERHORN, E. R. FULLER, J. MANDEL and A. G. EVANS, *J. Amer. Ceram. Soc.* **59** (1976) 403.
111. G. M. BUBEL, J. T. KRAUSE, B. J. BICKTA and R. T. KU, *J. Lightwave Technol.* **7** (1989) 1488.
112. EIA/TIA Standard 455-28B, "Method for measuring dynamic tensile strength of optical fibres", October (1991).
113. J. D. HELFINSTINE and F. QUAN, *Opt. Laser Techn.* **14** (1982) 133.
114. C. R. KURKJIAN, R. V. ALBARINO, J. T. KRAUSE et al., *Appl. Phys. (Lett.)* **28** (1976) 588.

Received 22 May  
and accepted 20 December 1994